Modulation Selection from a Battery Power Efficiency Perspective

Dongliang Duan, *Student Member, IEEE*, Fengzhong Qu, *Member, IEEE*,
Liuqing Yang, *Senior Member, IEEE*, Ananthram Swami, *Fellow, IEEE*, and Jose C. Principe, *Fellow, IEEE*

***Abstract*—In this paper, we compare the battery power efficiencies of various pulse-based modulations widely adopted for their low complexity. Taking into account circuit modules and battery imperfectness, we establish simple closed-form analytical formulas which can be used to conveniently determine the relative preference between arbitrary pulse-based modulation pairs in terms of their actual average battery energy consumption.**

***Index Terms*—Battery power efficiency (BPE), pulse-based modulations, nonlinear battery model.**

I. Introduction

BATTERY power efficiency (BPE) is a critical factor in modern wireless communication systems, especially for wireless sensor networks (WSNs) driven by nodes with non-renewable batteries [1]. Most literature on improving system power efficiency treats the batteries as ideal and linear, by assuming that all the battery's capacity can be fully utilized (see e.g., [2], [4], [6]). However, the empirically extracted battery models show that the actual battery discharge is a *nonlinear* process [5], [9]. Accordingly, using those nonlinear battery models has the potential to significantly improve the system lifetime [3].

The power efficiencies of modulations are already widely studied and well understood [7, Chapter 5]. However, these analyses often neglect the circuit system and battery inefficiency and the results are all based on the *spectral efficiency* rather than the *battery power efficiency*. In [11], a more realistic model for the transceiver nodes is proposed to study the BPEs of pulse-position modulation (PPM) and frequency-shift keying (FSK). In this model, circuit power consumptions, inefficiencies of power amplifier (PA) and DC/DC converter and nonlinear property of the battery power dissipation are considered. Under these more realistic considerations, [11] shows that, though considered to have the same spectral efficiency [7], the BPEs of PPM and FSK are actually very different and their relative BPE heavily relies upon the communication range and the system design criterion. Later, this same model is also adopted in [8] to analyze the BPEs of PPM and on-off keying (OOK) with imperfect channel state information. However, all these works heavily rely on the numerical analysis and no closed-form relationship has been established between the BPE comparison results and various system and modulation parameters. Moreover, these results are also limited to certain modulations and lack generality.

In this paper, we develop a general analytical framework to compare the BPEs between any pair of pulse-based modulations in *explicit closed form*. To do that, we take the difference between the actual average battery energy consumption (AABEC) per bit of different modulations. We show that the excessive battery energy consumption due to the nonlinear discharge process can be expressed explicitly as a function of the pulse shape and energy strength. In addition, we prove that this function is quadratic in the K-th power of the communication range, where K is the channel path-loss exponent. Based on properties of quadratic functions, we also exhaustively discuss all possible comparison outcomes. Specific comparison examples are also presented to validate our analysis and to illustrate our general result.

Paper approved by D. I. Kim, the Editor for Spread Spectrum Transmission and Access of the IEEE Communications Society. Manuscript received August 27, 2008; revised April 11, 2009, September 21, 2009, and December 10, 2009.

D. Duan, F. Qu, L. Yang, and J. C. Principe are with the Department of Electrical and Computer Engineering, University of Florida, P.O. Box 116130, Gainesville, FL 32611, USA (e-mail: {ddl85, jimqufz}@ufl.edu, lqyang@ece.ufl.edu, principe@cnel.ufl.edu).

A. Swami is with the Army Research Laboratory, 2800 Powder Mill Road, Adelphi, MD 20783 (e-mail: a.swami@ieee.org).

Parts of the results in this paper have been presented at IEEE Wireless Communications & Networking Conference, Budapest, Hungary, April 5-8, 2009. This work is in part supported by Office of Naval Research under grant #N00014-07-1-0868, and Army Research Office under Contract #W911NF-07-D-0001.

Digital Object Identifier 10.1109/TCOMM.2010.07.080443

II. System Model

A. Comparison Metric

In this paper, our metric of interest is battery power efficiency which we will simply call efficiency. Hence, we utilize the average actual battery energy consumption per bit as an indicator. The smaller it is, the more efficient the modulation is; and vice versa.

B. General Pulse-based Modulation Model

In this category of modulation schemes, the information bits are encoded in various characteristics of the transmitted pulse, such as the pulse presence, position, and shape etc. Here, we define a general model for the pulse-based modulation with the following parameters: 1) the pulse shape $p(t)$; 2) the pulse energy $\mathcal{E}_p$; 3) pulse duration T_p; 4) demodulation duration T_d depending on the modulation scheme; and 5) symbol duration T_s.

C. Path-Loss Channel Gain

The channel can be either deterministic or Rayleigh fading with additive white Gaussian noise (AWGN). In either case, the channel gain factor $G(d)$ depends on the transceiver distance d and is given by [10, Chapter 4]: $G(d) = \mathcal{P}_s/\mathcal{P}_r = M_l G_1 d^K$, where $\mathcal{P}_s$ and $\mathcal{P}_r$ are the transmitted and received power of the signal, and the remaining parameters are defined

in Table I. Accordingly, the relationship between the energy at the transmitter $\mathcal{E}$ and the energy at the receiver $\mathcal{E}_r$ is:

$$\mathcal{E}/\mathcal{E}_r = \mathcal{P}_s/\mathcal{P}_r = G(d) = M_l G_1 d^K \ . \tag{1}$$

D. Nonlinear Battery Model

As introduced in [11], the nonlinear behavior of the battery discharge process can be captured by $\mathcal{P}_0 = \int_{I_{\min}}^{I_{\max}} \frac{Vi}{\mu(i)} f(i) di$, where $\mathcal{P}_0$ is the average power consumption of the battery over a battery discharge process, V is the battery voltage, $f(i)$ is the density function of the battery discharge current profile during time period of interest $[t_{\min}, t_{max}]$, $\mu(i)$ is the *battery efficiency factor* [5] and $I_{\max}$ and $I_{\min}$ are respectively the maximum and minimum affordable discharge currents. To facilitate our ensuing analysis, we define the *instantaneous power consumption* at time t as $\mathcal{P}_0(t) = Vi(t)/\mu(i(t))$. Then, the average power consumption of the battery over the discharge interval $[t_{\min}, t_{\max}]$ can be alternatively expressed as:

$$\mathcal{P}_0 = \int_{t_{\min}}^{t_{\max}} \mathcal{P}_0(t) dt = \int_{t_{\min}}^{t_{\max}} \frac{Vi(t)}{\mu(i(t))} dt \ , \tag{2}$$

where ω is a positive parameter.

To describe the relationship between the battery efficiency factor $\mu(i)$ and the discharge current i, we adopt the empirical formula obtained in [5]:

$$\mu(i) = 1 - \omega i \ . \tag{3}$$

III. Average Actual Battery Energy Consumption Analysis

A. Transmitter Battery Energy Consumption

We obtain the actual battery energy consumption for transmitting a single pulse as the following lemma:

Lemma 1 *The total battery energy consumption for transmitting a single pulse $p(t)$ with duration T_p and energy $\mathcal{E}_p$ is approximately:*

$$\mathcal{E}_{0t} = \frac{\omega \gamma_p (1+\alpha)^2}{V \eta^2} \mathcal{E}_p^2 + \frac{1+\alpha}{\eta} \mathcal{E}_p + \frac{\mathcal{P}_{ct}}{\eta} T_p \ , \tag{4}$$

with parameters defined in Table I.

Proof: See Appendix A. ∎

In (4), η and α terms reflect the influence of the inefficiency of DC/DC converter[1] and the extra PA power loss on the battery energy consumption, respectively. Lemma 1 shows that the total battery energy consumption can be decomposed into three parts:

1) The first term in (4) refers to the excess power loss due to the nonlinear battery discharge process. This term is proportional to the square of the energy of the transmitted signal. In addition, this term is only affected by the pulse shape through a scaling factor γ_p. Notice that, though γ_p can be mathematically interpreted as the "energy" of $p_0(t)$, it is *not* the actual energy consumption of a DC battery with a constant voltage V. As detailed in Appendix A, the scaling factor γ_p is the result of normalization of the un-amplified pulse waveform $p_0(t)$ in order to ensure a constant *pure* (without any circuit energy consumption) and *ideal* (without any battery nonlinearity) battery energy consumption independent of the actual shape the pulse takes. Finally, this term also depends on the battery parameter ω, which captures the nonlinear feature of the battery.
2) The second term in (4) refers to the energy carried by the transmitted signal. If there were not effects of the DC/DC converter (via η) and the PA (via α), it would be exactly the energy of the transmitted pulse.
3) The third term in (4) refers to the circuit energy consumption. It depends on the power of the circuit and the pulse duration T_p.

[1]DC/DC converter matches the voltage level of the battery and the system circuit. If not used, $\eta = 1$, otherwise $\eta < 1$.

TABLE I
NOTATIONS

M_l	channel link margin
G_1	gain factor at $d = 1$
K	path-loss exponent
$\mu(i)$	battery efficiency factor $\mu(i) = 1 - \omega i$
η	transfer efficiency of the DC/DC converter
α	extra power loss factor of the PA
$p(t)$	transmitted pulse
γ_p	$\int_0^{T_p} \left(\frac{p(t)}{\int_0^{T_p} \lvert p(t) \rvert dt} \right)^2 dt$
$\mathcal{E}_p$	pulse energy
$\mathcal{E}_0$	average actual battery energy consumption (AABEC) per bit
$\mathcal{P}_{ct}$	transmitter circuit power
$\mathcal{P}_{cr}$	receiver circuit power
k_2	$\frac{M_l^2 G_1^2 \omega (1+\alpha)^2}{V \eta^2 M \log_2 M} \left(\sum_m \gamma_{p,m} \mathcal{E}_{pr,m}^2 \right)$
k_1	$\frac{M_l G_1 (1+\alpha)}{\eta M \log_2 M} \left(\sum_m \mathcal{E}_{pr,m} \right)$
k_0	$\frac{\mathcal{P}_{ct} \sum_m T_{p,m} + \mathcal{P}_{cr} \sum_m T_{d,m}}{\eta M \log_2 M}$
$\triangle$	$\left(k_1^{2\mathrm{v}1}\right)^2 - 4 k_2^{2\mathrm{v}1} k_0^{2\mathrm{v}1}$
r_1	$\frac{-k_1^{2\mathrm{v}1} + \sqrt{\left(k_1^{2\mathrm{v}1}\right)^2 - 4 k_2^{2\mathrm{v}1} k_0^{2\mathrm{v}1}}}{2 k_2^{2\mathrm{v}1}}$
r_2	$\frac{-k_1^{2\mathrm{v}1} - \sqrt{\left(k_1^{2\mathrm{v}1}\right)^2 - 4 k_2^{2\mathrm{v}1} k_0^{2\mathrm{v}1}}}{2 k_2^{2\mathrm{v}1}}$

B. Receiver Battery Energy Consumption

At the receiving node, there is no PA but a low noise amplifier (LNA) with nearly constant power consumption. Thus, the current $I_r = \mathcal{P}_{cr}/(\eta V)$ where $\mathcal{P}_{cr}$ is the circuit power consumption at the receiver. In general, I_r is very small, so $\mu(I_r) = 1 - \omega I_r \approx \mu_{\max} = 1$ [11]. The receiving circuit needs to be turned on for the demodulation duration T_d. Hence, the total battery energy consumption of the receiving

node is:

$$\mathcal{E}_{0r} = \frac{\mathcal{P}_{cr}}{\eta} T_d \ . \tag{5}$$

C. Average Actual Battery Energy Consumption of Modulation Schemes

Taking into account the path-loss effect of the channel in Section II-C, we establish the relationship between the AABEC of the modulation scheme and the transmission distance as follows:

Theorem 1 *The AABEC per bit for a modulation scheme is a quadratic function of d^K, where d is the transmission distance and K is the path loss exponent, i.e.:*

$$\mathcal{E}_0(d) = k_2 \left(d^K\right)^2 + k_1 d^K + k_0 \tag{6}$$

with parameters defined in Table I.

Proof: See Appendix B. ■

IV. General Comparison Result

With Theorem 1, we will now look at the energy consumption difference for different modulation schemes to see how their energy consumptions compare when transmitting at the same rates while achieving identical system performance. The AABEC difference between any two pulse-based modulations is given by:

$$\begin{aligned} \mathcal{E}_D^{2\text{v}1}(d) &= (k_2^2 - k_2^1)\left(d^K\right)^2 + (k_1^2 - k_1^1)d^K + (k_0^2 - k_0^1) \\ &= k_2^{2\text{v}1}\left(d^K\right)^2 + k_1^{2\text{v}1} d^K + k_0^{2\text{v}1} \ , \end{aligned} \tag{7}$$

where the subscript D means "difference" and the superscripts 1 and 2 each refers to a modulation scheme in comparison.

It is evident according to Theorem 1 that the AABEC difference is in a simple quadratic form in d^K and the sign of a quadratic function can be determined by the discriminant $\triangle = \left(k_1^{2\text{v}1}\right)^2 - 4k_2^{2\text{v}1}k_0^{2\text{v}1}$ and the roots (when $\triangle > 0$) $r_1 = \left(-k_1^{2\text{v}1} + \sqrt{\left(k_1^{2\text{v}1}\right)^2 - 4k_2^{2\text{v}1}k_0^{2\text{v}1}}\right) / \left(2k_2^{2\text{v}1}\right)$ and $r_2 = \left(-k_1^{2\text{v}1} - \sqrt{\left(k_1^{2\text{v}1}\right)^2 - 4k_2^{2\text{v}1}k_0^{2\text{v}1}}\right) / \left(2k_2^{2\text{v}1}\right)$. From the properties of quadratic functions, we can obtain the following result:

Result 1 *The relative efficiency between two modulation schemes must follow one and only one of the following cases:*

- *C1 One modulation scheme is always more efficient than the other. This occurs when r_1 and r_2 are both negative.*
- *C2 One modulation scheme is more efficient when $d < d_c^{2v1}$ and the other is more efficient when $d > d_c^{2v1}$, where $d_c^{2v1} = \max(r_1, r_2)$. This occurs when $\triangle > 0$ with $r_1 r_2 < 0$.*
- *C3 One modulation scheme is more efficient when $d \in (d_{c1}^{2v1}, d_{c2}^{2v1})$, and the other is more efficient otherwise, where $d_{c1}^{2v1} = \min(r_1, r_2)$ and $d_{c2}^{2v1} = \max(r_1, r_2)$. This occurs when $\triangle > 0$ with r_1 and r_2 both positive.*

Here, d_{c*}^*s refer to critical distances at which the relative battery efficiency of modulations changes sign.

TABLE II
Simulation Parameters

$\omega = 0.05$	$T_p = 1.33 \times 10^{-4}$s	$\alpha = 0.33$	$\mu_{\min} = 0.5$
$K = 3$	$N_0/2 = -171$dBm/Hz	$G_1 = 27$dB	$M_l = 40$dB
$V = 3.7$V	$\mathcal{P}_{cr} = 52.5$mW	$\mathcal{P}_{ct} = 105.8$mW	$\eta = 0.8$

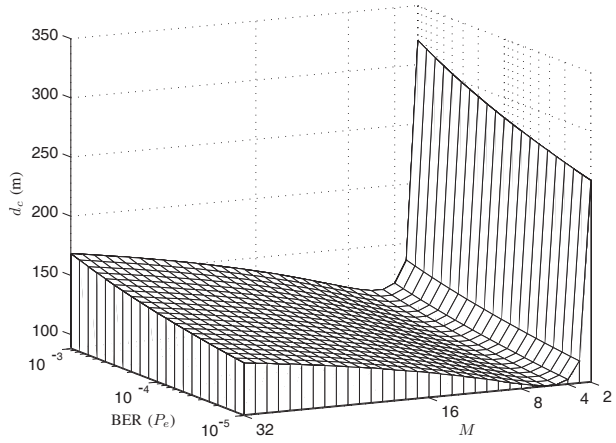

Fig. 1. Comparison results of M-PPM and OOK under deterministic AWGN channel as a function of PPM modulation size M and BER requirement. Below the surface: OOK-advantageous region; above the surface: PPM-advantageous region.

V. Numerical Analysis with Specific Comparison Pairs

From Section IV, we see that all possible forms of BPE comparison result in an explicit closed form. In this section, the numerical analysis for specific comparison pairs are obtained through Result 1. The parameters used in the numerical plots are listed in Table II [2], [11]. For fair comparisons, we ensure that each modulation pair has identical bandwidth occupancy and bandwidth efficiency while achieving the same bit error rate (BER) performance.

A. OOK and M-PPM under Deterministic AWGN Channel

As discussed in [8], OOK and M-PPM need to use the same pulse $p(t)$ with duration T_p for same bandwidth occupancy and OOK needs to be duty cycled to guarantee the same bandwidth efficiency. When compared with M-PPM, the OOK duty cycling factor is $\frac{\log_2 M}{M}$ and thus for OOK, $T_d^O = T_p = \frac{\log_2 M}{M} T_s^O$. For M-PPM, $T_d^P = T_s^P = MT_p$. Without loss of generality, we use the rectangular pulse in base band. Hence, $\gamma_{pr,0}^O = 0$ and $\gamma_{pr,1}^O = \gamma_{pr,m}^P = 1/T_p$ for any m.

In AWGN channels, the symbol energies $\mathcal{E}_b^O$ and $\mathcal{E}_b^P$ to achieve certain prescribed BER P_e are readily available through existing formulas [7]. Plugging in all the parameters in Table I, we will find that the comparison results falls under C2 in Result 1. Accordingly, the preference region is plotted in Fig. 1.

The closed-form expressions for the critical transmission distances are neat and convenient to use in real applications. However, in the derivation process, we used the approximation $\omega i(t) \ll 1$, where $i(t)$ is the instantaneous current drawn

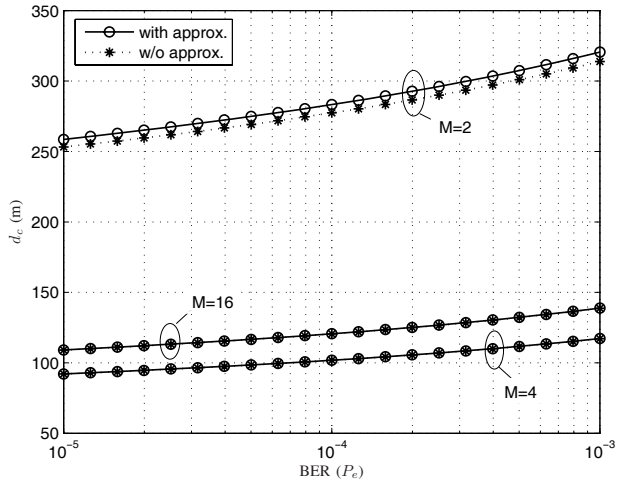

Fig. 2. Comparison of d_c obtained by our closed form expression and via numerical search.

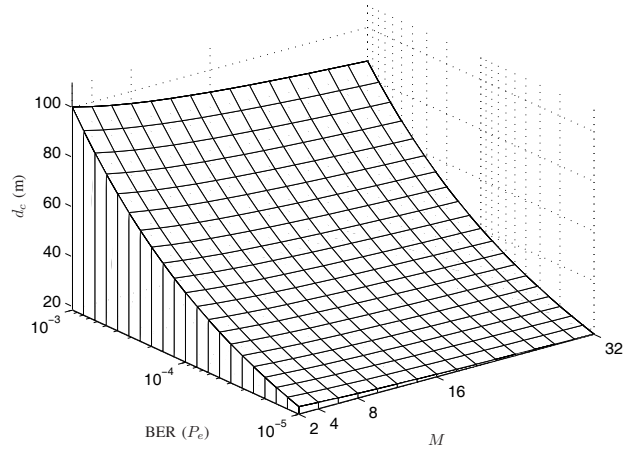

Fig. 3. Comparison results of M-FSK and M-PPM under Rayleigh fading channel as a function of modulation size M and BER requirement. Below the surface: PPM-advantageous region; above the surface: FSK-advantageous region.

from the battery. To verify the validity of this approximation, from Fig. 2, we see that our results with approximation (solid line with circle) are quite accurate when compared with the results obtained by numerical search without any approximation (dotted line with star).

B. M-FSK and M-PPM under Rayleigh Fading Channel

Treating the carriers with different frequencies as pulse shapers, we can consider M-FSK as a pulse-based modulation scheme with information embedded in the shape of the pulse. The signal pulse transmitted for symbol $m \in \{0, 1, \ldots, M-1\}$ is $p_m^F(t) = \sin(2\pi(f_c + (2m-1)\triangle f)t), t \in [0, T_s]$, where f_c is the central carrier frequency and $\triangle f$ is the frequency spacing.

For M-PPM, all possible signals utilize the same pulse shaper and the information is conveyed by the signal position. To compare with M-FSK, we take the pulse in pass band, then the basic pulse is $p^P(t) = \sin 2\pi f_c t$ with $t \in [0, T_s/M]$, where f_c is the carrier frequency. Correspondingly, the pulse transmitted for symbol m is $p_m^P(t) = p^P\left(t - m\frac{T_s}{M}\right)$.

It is shown in [11] that with $\triangle f = 1/T_s$, M-FSK and M-PPM have identical bandwidth occupancy and bandwidth efficiency. Hence, no duty cycling is needed. For both modulation schemes, $T_d^F = T_d^P = T_s$.

To compare these two modulation schemes, we need to first obtain the pulse shape factors γ_p^F and γ_p^P. According to Section II-B and Lemma 1, for M-FSK:$\gamma_{p,m}^F = \frac{\int_0^{T_s}[\sin(2\pi(f_c+(2m-1)\triangle f)t)]^2 dt}{\left[\int_0^{T_s}|\sin[2\pi(f_c+(2m-1)\triangle f)t]|dt\right]^2} = \frac{T_s}{2}/\left(\frac{T_s}{2\pi}\right)^2 = \frac{2\pi^2}{T_s}$. Similarly, for M-PPM, we have $\gamma_{p,m}^P = \frac{2\pi^2}{T_s/M} = M\frac{2\pi^2}{T_s} = M\gamma_{p,m}^F$.

PPM and FSK have the same required energy at the receiver, i.e., $\mathcal{E}_{pr}^F = \mathcal{E}_{pr}^P = \mathcal{E}_{sr}$, where $\mathcal{E}_{sr}$ is the required average symbol energy to get the objective BER performance P_e. In Rayleigh fading channels, this value can be obtained from the formula given in [11].

Substituting all these parameters into Table I, we obtain $k_2^{\text{FvP}} = (1-M)\frac{2\pi^2 M_l^2 G_1^2 \omega(1+\alpha)^2}{T_s V \eta^2 \log_2 M}\mathcal{E}_{sr}^2 < 0, k_1^{\text{FvP}} = 0, k_0^{\text{FvP}} = \frac{M-1}{M^2}\frac{\mathcal{P}_{ct}T_s}{\eta \log_2 M} > 0$. Accordingly, the comparison between PPM and FSK also falls under C2 in Result 1 and the preference region is plotted in Fig. 3.

Interestingly, although $\omega i(t) \ll 1$ as used in our analysis and verified in Section V-A, the comparison between M-PPM and M-FSK here shows that this slight nonlinearity of the battery is actually *not* negligible. If no battery nonlinearity were considered, then we would expect that M-PPM is always preferred since it costs less transmitter circuit power consumption. However, comparison result shows that M-FSK is preferred when transmission distance is sufficiently large.

In addition, for most communication systems in real applications, the critical transmission distances given by Fig. 1 and Fig. 3 are within the typical transmission distance (for example, typical transmission distance of wireless sensor networks is around 10 to 1000 meters). This confirms that our neat analytical formulas have practical values in real applications.

VI. Conclusions

In this paper, we compared pulse-based modulations from the battery power efficiency perspective. First, we adopted the realistic nonlinear battery model and took into account all common power consumption factors in the system model. Then, we analyzed the battery power efficiency between arbitrary modulation pairs and found that the comparison results can be characterized by the transmission distances in an explicit closed form. The numerical comparison examples are presented to validate our analysis and to illustrate our result.

Appendix A
Proof of Lemma 1

Denote the output current as $p(t)$.[2]. Then, at the output stage, the total energy consumption $\mathcal{E}_o$ can be obtained as $\mathcal{E}_o = \int_0^{T_p} V\,|p(t)|\,dt$. Due to the inefficiency of the DC/DC

[2]In this paper, we assume PA of type AB is used. Thus the output current has the same shape as the pulse $p(t)$. If PA of other type is used, the current may take a distorted shape $p'(t)$. Accordingly, the γ_p in this lemma should be replaced by $\gamma_{p'}$ calculated by the distorted pulse shape $p'(t)$.

converter and the extra power loss of the power amplifier, the output pulse energy is $\mathcal{E}_p = \eta\mathcal{E}_o/(1+\alpha)$. Define $p_0(t) = p(t)/\int_0^{T_p}|p(t)|\,dt$, then $p(t) = \frac{(1+\alpha)\mathcal{E}_p}{\eta V}p_0(t)$. In addition to the current induced by the transmitted waveform, the circuit power consumption will also induce a current $I_{ct} = \mathcal{P}_{ct}/(\eta V)$. Thus, the instantaneous current running through the battery is $i(t) = |p(t)| + I_{ct}$. From (2), we can obtain the total battery energy consumption in one pulse duration as follows:

$$\begin{aligned}
\mathcal{E}_{0t} &= \int_0^{T_p}\mathcal{P}_0(t)dt = \int_0^{T_p}\frac{Vi(t)}{\mu(i(t))}dt \\
&= V\int_0^{T_p}\frac{i(t)}{1-\omega i(t)}dt \approx V\int_0^{T_p} i(t)(1+\omega i(t))dt \\
&= V\int_0^{T_p}(|p(t)|+I_{ct})\left[1+\omega(|p(t)|+I_{ct})\right]dt \\
&= V\left[(1+2\omega I_{ct})\int_0^{T_p}|p(t)|\,dt+(1+\omega I_{ct})\int_0^{T_p}I_{ct}dt+\omega\int_0^{T_p}(p(t))^2dt\right] \\
&\approx V\left[\int_0^{T_p}|p(t)|\,dt+\int_0^{T_p}I_{ct}dt+\omega\int_0^{T_p}(p(t))^2dt\right] \\
&= V\left[\frac{(1+\alpha)\mathcal{E}_p}{\eta V}+\frac{\mathcal{P}_{ct}}{\eta V}T_p+\omega\frac{(1+\alpha)^2\mathcal{E}_p^2}{\eta^2V^2}\gamma_p\right] \\
&= \frac{\omega\gamma_p(1+\alpha)^2}{\eta^2V}\mathcal{E}_p^2+\frac{1+\alpha}{\eta}\mathcal{E}_p+\frac{\mathcal{P}_{ct}}{\eta}T_p\ ,
\end{aligned}$$

where substitution $\gamma_p := \int_0^{T_p}(p_0(t))^2dt$ is used. In the above derivation, the first approximation comes from the fact that practically $\omega i(t) \ll 1$, and thus $1/(1-\omega i(t)) \approx 1+\omega i(t)$, and the second approximation follows from $\omega I_{ct} \ll 1$.

APPENDIX B
PROOF OF THEOREM 1

From (4) and (5), we see that the total battery energy consumption for one pulse communication is:

$$\mathcal{E}_{0p} = \mathcal{E}_{0t}+\mathcal{E}_{0r} = \frac{\omega\gamma_p(1+\alpha)^2}{V\eta^2}\mathcal{E}_p^2+\frac{1+\alpha}{\eta}\mathcal{E}_p+\frac{\mathcal{P}_{ct}T_p+\mathcal{P}_{cr}T_d}{\eta}$$

As introduced in Section II-B, a modulation scheme with size M will choose from M pulses to transmit $\log_2 M$ bits of information, so the average actual battery energy consumption per bit transmission is:

$$\begin{aligned}
\mathcal{E}_0 &= \frac{1}{\log_2 M}\frac{1}{M}\sum_m \mathcal{E}_{0p,m} \\
&= \frac{1}{M\log_2 M}\sum_m \\
&\left[\frac{\omega\gamma_{p,m}(1+\alpha)^2}{V\eta^2}\mathcal{E}_{p,m}^2+\frac{1+\alpha}{\eta}\mathcal{E}_{p,m}+\frac{\mathcal{P}_{ct}T_{p,m}+\mathcal{P}_{cr}T_{d,m}}{\eta}\right]
\end{aligned}$$

where the subscript $m \in \{0,1,\ldots,M-1\}$ refers to the symbol transmitted.

Notice that from (1), $\mathcal{E}_{p,m} = M_l G_1 d^K \mathcal{E}_{pr,m}$, thus:

$$\begin{aligned}
\mathcal{E}_0 = &\left[\frac{M_l^2G_1^2\omega(1+\alpha)^2}{V\eta^2M\log_2 M}\left(\sum_m\gamma_{p,m}\mathcal{E}_{pr,m}^2\right)\right]d^{2K} \\
&+\left[\frac{M_lG_1(1+\alpha)}{\eta M\log_2 M}\left(\sum_m\mathcal{E}_{pr,m}\right)\right]d^K \\
&+\frac{\mathcal{P}_{ct}\sum_m T_{p,m}+\mathcal{P}_{cr}\sum_m T_{d,m}}{\eta M\log_2 M}.
\end{aligned}$$

This is a quadratic function of d^K and the coefficients are as stated in Theorem 1.

REFERENCES

[1] I. F. Akyildiz, W. Su, Y. Sankarasubramaniam, and E. Cayirci, "A survey on sensor networks," *IEEE Commun. Mag.*, vol. 40, no. 8, pp. 102-114, Aug. 2002.

[2] S. Cui, A. J. Goldsmith, and A. Bahai, "Energy-constranined modulation optimization," *IEEE Trans. Commun.*, vol. 4, no. 5, pp. 2349-2360, Sep. 2002.

[3] K. Lahiri, A. Raghunathan, S. Dey, and D. Panigrahi, "Battery-driven system design: a new frontier in low power design," in *Proc. Intnl. Conf. VLSI Design*, Bangalore, India, Jan. 2002, pp. 261-267.

[4] J. N. Laneman, D. N. C. Tse, and G. W. Wornell, "Cooperative diversity in wireless networks: efficient protocals and outage behavior," *IEEE Trans. Inf. Theory*, vol. 50, no. 12, pp. 3062-3080, Dec. 2004.

[5] M. Pedram and Q. Wu, "Battery-powered digital CMOS design," *IEEE Trans. VLSI Syst.*, vol. 10, no. 5, pp. 601-607, Oct. 2002.

[6] Y. Prakash and S. K. S. Gupta, "Time to failure estimation for batteries in portable systems," in *Proc. Wireless Commun. Netw. Conf.*, New Orleans, LA, Mar. 2003, pp. 212-217.

[7] J. Proakis, *Digital Communications*, 4th edition. New York: McGraw-Hill, Feb. 2001.

[8] F. Qu, D. Duan, L. Yang, and A. Swami, "Signaling with imperfect channel state information: a battery power efficiency comparison," *IEEE Trans. Signal Process.*, vol. 56, no. 9, pp. 4486-4495, Sep. 2008.

[9] D. Rakhmatov and S. Vrudhula, "Time to failure estimation for batteries in portable systems," in *Proc. International Symp. Low Power Electron. Design*, Huntington Beach, CA, USA, Aug. 2001, pp. 88-91.

[10] T. S. Rappaport, *Wireless Communications: Principles and Practice*, 2nd edition. Prentice-Hall, 2002.

[11] Q. Tang, L. Yang, G. B. Giannakis, and T. Qin, "Battery power efficiency of PPM and FSK in wireless sensor networks," *IEEE Trans. Commun.*, vol. 6, no. 4, pp. 1308-1319, Apr. 2007.